

OPEN ACCESS

EDITED BY

Niyaz Ahmed,
University of Hyderabad, India

REVIEWED BY

Vipin Rana,
University of Maryland, College Park,
United States
Fan Zhang,
Louisiana State University, United States

*CORRESPONDENCE

Wei-Kun Zeng
✉ zengweikun@126.com

SPECIALTY SECTION

This article was submitted to
Microbial Immunology,
a section of the journal
Frontiers in Immunology

RECEIVED 19 December 2022

ACCEPTED 27 March 2023

PUBLISHED 12 April 2023

CITATION

Ding A-J, Zhang W-M, Tao J, Chen B,
Liu X-C, Dong Y, Ma H-J, Pan S-D, He J-B
and Zeng W-K (2023) *Salmonella enterica*
serovar Paratyphi A-induced immune
response in *Caenorhabditis elegans*
depends on MAPK pathways and DAF-16.
Front. Immunol. 14:1118003.
doi: 10.3389/fimmu.2023.1118003

COPYRIGHT

© 2023 Ding, Zhang, Tao, Chen, Liu, Dong,
Ma, Pan, He and Zeng. This is an open-
access article distributed under the terms of
the [Creative Commons Attribution License
\(CC BY\)](https://creativecommons.org/licenses/by/4.0/). The use, distribution or
reproduction in other forums is permitted,
provided the original author(s) and the
copyright owner(s) are credited and that
the original publication in this journal is
cited, in accordance with accepted
academic practice. No use, distribution or
reproduction is permitted which does not
comply with these terms.

Salmonella enterica serovar Paratyphi A-induced immune response in *Caenorhabditis elegans* depends on MAPK pathways and DAF-16

Ai-Jun Ding, Wei-Ming Zhang, Jian Tao, Bing Chen,
Xiao-Cao Liu, Yu Dong, Han-Jing Ma, Shao-Dong Pan,
Jiang-Bo He and Wei-Kun Zeng*

School of Medicine, Kunming University, Kunming, China

Salmonella enterica serovar Paratyphi A (*S. Paratyphi A*) is a pathogen that can cause enteric fever. According to the recent epidemic trends of typhoid fever, *S. Paratyphi A* has been the major important causative factor in paratyphoid fever. An effective vaccine for *S. Paratyphi A* has not been developed, which made it a tricky public health concern. Until now, how *S. Paratyphi A* interacts with organisms remain unknown. Here using lifespan assay, we found that *S. Paratyphi A* could infect *Caenorhabditis elegans* (*C. elegans*) at 25°C, and attenuate thermotolerance. The immune response of *C. elegans* was mediated by *tir-1*, *nsy-1*, *sek-1*, *pmk-1*, *mpk-1*, *skn-1*, *daf-2* and *daf-16*, suggesting that *S. Paratyphi A* could regulate the MAPK and insulin pathways. Furthermore, we observed several phenotypical changes when *C. elegans* were fed *S. Paratyphi A*, including an accelerated decline in body movement, reduced the reproductive capacity, shortened spawning cycle, strong preference for OP50, arrested pharyngeal pumping and colonization of the intestinal lumen. The virulence of *S. Paratyphi A* requires living bacteria and is not mediated by secreting toxin. Using hydrogen peroxide analysis and quantitative RT-PCR, we discovered that *S. Paratyphi A* could increase oxidative stress and regulate the immune response in *C. elegans*. Our results sheds light on the infection mechanisms of *S. Paratyphi A* and lays a foundation for drugs and vaccine development.

KEYWORDS

Salmonella enterica serovar Paratyphi A, *Caenorhabditis elegans*, MAPK, oxidative stress, immune

Introduction

Salmonella enterica serovar Paratyphi A (*S. Paratyphi A*) is the causative pathogen of paratyphoid fever and accompanied with fever, abdominal pain, diarrhea, nausea and sometimes vomiting or in extreme cases, it can lead to life-threatening systemic disease (1, 2). In China, the incidence of *S. Paratyphi A* is estimated to range from 0.08 to 192.5 cases for

every 100,000 person per year (3). And among the causative pathogen of enteric fever, *S. Paratyphi A*'s share ranges from 0.6 to 98.7% (4). The Southeast Asia region presents the third highest incidence of *S. Paratyphi A*-associated infections worldwide, and the incidence of typhoid fever is approximately 110 cases/100 000 population every year (5). Moreover, the occurrence of *S. Paratyphi A* infection has presented a sudden increase in Rourkela, western Odisha (6). A recent report suggested that *S. Paratyphi A* has already spread to countries worldwide (7), which indicates that infection with *S. Paratyphi A* has become a major public health problem. These days, vaccination development for *S. Paratyphi A* focuses on live attenuated vaccines (8, 9), subunit vaccines (10, 11) and conjugate vaccines (12, 13). However, an effective parathyroid vaccine has not been developed. And fluoroquinolones, ciprofloxacin, third generation cephalosporins, nalidixic acid and pefloxacin-resistant *S. Paratyphi A* are gradually increasing (2, 14–17). Therefore, the pathogenic mechanism of *S. Paratyphi A* must be elucidated.

As an invertebrate model, *Caenorhabditis elegans* possess similar host-microbe interactions to the human gut. The virulence and innate immune mechanisms caused by pathogen were reported conserved between *C. elegans* and mammals (18). The human pathogen, such as *Salmonella enterica*, can also infect and lead to pathogenicity in *C. elegans* (19). What's more, *C. elegans* is known to share conserved defense mechanisms against pathogenic infection (20). Unlike the highly intricate immune network of vertebrates, the original signal network of *C. elegans* make it easier to clarify the relationship among immune signals.

The MAPK pathways, such as PMK-1/p38 MAPK and MPK-1/ERK MAPK, play a major role in defending against pathogens in *C. elegans*, and MAPK mutants are more sensitive to pathogens (21, 22). Among the immune pathways, Insulin/insulin-like growth factor 1 (IGF-1) signaling (IIS) is conserved in various species. Inhibition of IIS, could induce longevity and improve survival on pathogens (23) and activate DAF-16/FOXO, which is an important transcription factor regulating immune response and stress resistance related genes (24). DAF-16 is not just a target gene of IIS, but also a key molecule to integrate signals from other pathways such as oxidative stress to induce transcriptional changes involved in immunity, stress, and metabolism related genes (25). SKN-1, the other immune-related transcription factor acting the downstream of MAPK pathway and oxidative stress, plays an essential role in detoxification in immunity (26, 27). Despite extensive research on immune pathways, which immune pathways participate in *S. Paratyphi A* infection remains unknown.

Here, we modeled *C. elegans* infection with *S. Paratyphi A*, and found that *S. Paratyphi A* could shorten the lifespan and change thermotolerance and reproductive capacity and spawning cycle and pharyngeal pumping and body movement of *C. elegans*. As secretions and heat-killed treatment of *S. Paratyphi A* exhibited avirulent, *S. Paratyphi A* might infect *C. elegans* by colonizing the intestinal lumen. Hydrogen peroxide assays indicated that *S. Paratyphi A* infection could induce oxidative stress in *C. elegans*. Our results of quantitative RT-PCR indicated that the stress response was changed when worms were fed *S. Paratyphi A*. Genetic analysis with a series of *C. elegans* mutants showed that worms defend against *S. Paratyphi A* via the MAPK pathways and DAF-16. The study elucidated some infection

mechanisms of *S. Paratyphi A* and may contribute to the development of drugs and vaccines.

Materials and methods

C. elegans and bacterial strains

The wild-type N2, PS3551 *hsf-1(sy441) I*, ZD101 *tir-1(qd4) III*, AU3 *nsy-1(ag3) II*, KU4 *sek-1(km4) X*, KU25 *pmk-1(km25) IV*, BJS737 *mpk-1(sbj10) III*, CB1370 *daf-2(e1370) III*, CF1038 *daf-16(mu86)I*, EU1 *skn-1(zu67)IV* and TJ356 zIs356 [*daf-16p::daf-16a/b::GFP +rol-6(su1006)*] *C. elegans* strains were provided by the *Caenorhabditis* Genetics Center (CGC) and grown at the 25°C (PS3551 *hsf-1(sy441) I* and CB1370 *daf-2(e1370) III* were grown at 20°C) (28). Worms were maintained on NGM plates containing *Escherichia coli* OP50. *E. coli* OP50 and HT115 were procured from CGC, *E. coli* strain JM109 was purchased from Promega Corporation and all grown in Luria-Bertani (LB) medium. Clinical isolates of *Salmonella enterica* serovar Paratyphi A CMCC50973 were provided by the National Center for Medical Culture Collections (Beijing, China) and cultivated in LB broth at 37°C. We constructed the *E. coli::eGFP* and *S. Paratyphi A::eGFP* (both carry the same eGFP expression plasmid pMD18T-*egfp*).

Lifespan assay

For the wild-type N2 lifespan assay at 25°C, synchronized L4 larvae N2 worms were washed with PBS and then grown on NGM plates containing *S. Paratyphi A* or *E. coli* OP50 and other *E. coli* strains (HT115 and JM109). In the spawning cycle, the nematodes were picked up by wormpicker to new plates every other day as previously described (29).

For the mutant strain lifespan assay, Late L4 larvae N2 worms and mutants were washed with PBS and maintained to NGM plates containing OP50 or *S. Paratyphi A*. Nematodes were picked and transferred to fresh plates with OP50 or *S. Paratyphi A* every other day. Worms were determined as dead if they showed non-response to a mechanical stimulus. Worms were excluded if they leaved plate, appeared swelling of internal organs, or hatched progeny in the maternal worms. The data of lifespan were analyzed by using IBM SPSS version 19.0. Kaplan–Meier lifespan analysis was applied, and log-rank test was carried out to calculate *p* values. The effects of OP50 and *S. Paratyphi A* on the mutant *C. elegans* were analyzed using Cox proportional-hazard models (30). The most obvious results of three independent trials are shown in the curves. Mean lifespan of at least 3 independent experiments are displayed as the mean ± standard deviation. * *p* < 0.05, ** *p* < 0.01, and *** *p* < 0.001 represented three levels of statistical significance when using Student's *t*-test.

Thermotolerance assay

To eliminate the effects of reproduction, the thermotolerance assays were performed with hermaphrodites on adult day 5, about

the time that egg-laying had finished (31). Briefly, synchronized day 5 worms fed OP50 were washed with PBS and cultivated onto plates with OP50 or *S. Paratyphi A* and incubated at 35°C. Survival was determined every 2 h at 35°C. Kaplan–Meier lifespan analysis was applied, and log-rank test was carried out to calculate *p* values. The most obvious results of three independent trials are shown in the curves. Mean lifespan of at least 3 independent experiments are presented as the mean \pm standard deviation. * *p* < 0.05, ** *p* < 0.01, and *** *p* < 0.001 represented three levels of statistical significance when using Student's *t*-test.

Body movement assay

Body movement assays were carried out as reported previously (32). To eliminate the influence by thickness of the bacterial lawn on OP50 or *S. Paratyphi A*, and considering that OP50 grow slowly, the assay was performed with bacteria at density of 5×10^9 and 5×10^{10} bacteria/mL for OP50 group and 5×10^9 bacteria/mL for *S. Paratyphi A* group. Overnight cultures of OP50 and *S. Paratyphi A* were separately inoculated 1:100 into fresh LB broth. After maintained in a shaker (200 rpm) at 37°C for about 3.5 h, the cultures were stored at 4°C. Serial dilution of cultures was spread on LB plates to determine the bacterial count. According to the counts, dilution or concentration by centrifuge were done to adjust the final concentration as OP50 5×10^9 /mL, OP50 5×10^{10} /mL and *S. Paratyphi A* 5×10^9 /mL. 200 μ L of each bacteria density was added onto 6 cm NGM plates. Then synchronized L4 larvae N2 worms were washed with PBS to remove OP50 and then cultivated to NGM plates containing OP50 or *S. Paratyphi A*. *C. elegans* were at fast moving stages when they crawled continuously in a well-coordinated sinusoidal curve pattern after tapping the plate, otherwise, the worms were defined as a not fast movement. The movement of worms was scored daily. The data of body movement were analyzed by using IBM SPSS version 19.0. Kaplan–Meier analysis was applied, and log-rank test was carried out to calculate *p* values. At least three independent experiments were carried out, and the most obvious result is shown in the curves. Data are presented as the mean \pm standard deviation from three independent experiments. * *p* < 0.05, ** *p* < 0.01, and *** *p* < 0.001 represented three levels of statistical significance when using Student's *t*-test.

Spawning assay

To analyze the effect of *S. Paratyphi A* on the spawning of *C. elegans*, eggs of N2 worms were grown on plates containing OP50 or *S. Paratyphi A* and incubated at 25°C, and 15 L4 larvae N2 worms were transferred to a new plate every day until eggs laying finished. The number of progenies produced by a specific worm was counted throughout the spawning cycle through everyday interval. The assay was performed in at least three independent trials, and all the results are displayed in this study.

Chemotaxis assay

To assess food preference in the presence of OP50 or *S. Paratyphi A* on the same plate, chemotaxis assays were performed

as previously reported (33). 25 μ L of each bacterial suspension was seeded within a circle with diameter of 2 cm on either end of a 60 mm NGM plate, worms were placed to center of the plate where is 1 cm away from the test bacterial spots. Synchronized L4 larvae N2 worms were washed with PBS and trained to NGM plates containing OP50 or *S. Paratyphi A* at 25°C for 12 h. Then, the animals were washed off the training plates in PBS and washed two more times in PBS. Using a wide orifice tip, 20 μ L of PBS containing approximately 50–100 nematodes were added to the plate midway between OP50 and *S. Paratyphi A* lawns. The plates were incubated at 25°C for 1 h before analyzing the number of animals on each zone. The chemotaxis index was calculated based on the formula: Chemotaxis index = (No. of worms on OP50 lawn–No. of worms on *S. Paratyphi A* lawn)/Total No. of worms tested. The assay was carried out at least three independent trials, and all the results are displayed in this study.

Pharyngeal pumping assay

To check the feeding behavior of worms exposed to OP50 and *S. Paratyphi A*, at least 10 synchronized L4 larvae N2 worms were transferred to plates seeded with OP50 or *S. Paratyphi A* and grown at 25°C. The pharyngeal pumping rates of OP50 or *S. Paratyphi A*-exposed nematodes were analyzed at 12 h, 24 h, and 48 h using a stereomicroscope for 20 seconds duration.

Bacterial colonization assay

The bacterial colonization assay was carried out according to previous reports (34, 35). Age-synchronized L4 larvae N2 worms were washed with PBS and grown on plates seeded with OP50 or *S. Paratyphi A* for 12 h, 24 h, and 48 h at 25°C. Then 10 worms were washed with PBS containing 25 mM levamisole (to stop pharyngeal pumping) and then immersed in 100 μ g/mL gentamicin and 25 mM levamisole for 1 h to clear the bacteria on the surface of nematodes and then washed twice more with PBS alone. Then worms were transferred to plates without any food to further remove the antibiotics and bacteria. 10 worms were picked up immediately and disrupted mechanically in 50 μ L of PBS containing 1% Triton X-100 in 1.5 mL Eppendorf tube. The worm lysates were diluted in PBS and plated on MacConkey agar at 37°C. After overnight incubation, OP50 and *S. Paratyphi A* colonies were counted and the CFU/worm was calculated.

Analysis of live bacterial accumulation in intestinal lumen

To confirm that *S. Paratyphi A* could proliferate in the intestinal lumen, synchronized L4 larvae N2 worms grown on OP50 seeded plates were transferred to plates containing *E. coli::eGFP* or *S. Paratyphi A::eGFP*. After ingestion of *E. coli::eGFP* or *S. Paratyphi A::eGFP* for 24 hours, the nematodes were rinsed three more times in PBS to remove residual bacteria and subsequently

grown on NGM plates without any bacteria, where they fasted for 24 hours until the fluorescence analysis were carried out (36). The fluorescence microscope system (Life Technologies EVOS FL Auto) was used to detect fluorescence in the intestine under 100-fold magnification.

Bacterial viability and secretions assay

After overnight growth, *E. coli* OP50 and *S. Paratyphi A* were inactivated at 65°C for 30 min (37). Then the cultures of OP50 and *S. Paratyphi A* were incubated on MacConkey agar at 37°C to check whether any bacteria survived. Synchronized L4 larvae N2 worms were added to plates seeded with heat-killed *E. coli* OP50 or *S. Paratyphi A*, lifespan assay was performed as described above.

To examine whether the secretions of *S. Paratyphi A* affect the viability of *C. elegans*, we carried out secretions assay as previously reported (38). After overnight growth, cultures of OP50 and *S. Paratyphi A* were centrifuged at 5,000 g for 10 min. 0.22 µm syringe filter was used to clear residual bacteria of the supernatant. Heat-killed *E. coli* OP50 were resuspended in the filtered supernatant and added to NGM plates. Then lifespan assay of N2 worms was carried out.

Subcellular localization of DAF-16/FOXO assay

Synchronized L4 stage of strain TJ356 zIs356 [*daf-16p::daf-16a/b::GFP + rol-6(su1006)*] were washed with PBS and maintained on plates containing OP50 or *S. Paratyphi A* for 30 min at 25°C. The fluorescence microscope system (Life Technologies EVOS FL Auto) was applied to test the subcellular localization of DAF-16 under 200-fold magnification.

Hydrogen peroxide assay

Synchronized L4 larvae N2 worms were rinsed with PBS and grown on plates seeded with OP50 or *S. Paratyphi A* for 12, 24 and 48 hours. Worms were washed with PBS and disrupted mechanically. The concentration of protein was quantified with a BCA Protein Assay Kit (Beyotime) for different times. At the same time, the hydrogen peroxide was tested using Hydrogen Peroxide (H₂O₂) Content Assay Kit (Solarbio). The data were expressed as µM hydrogen peroxide generation/mg of proteins.

Quantitative RT-PCR assays

Synchronized L4 larvae N2 worms were collected and washed with PBS to exhaust residual bacteria and then grown on plates with OP50 or *S. Paratyphi A* for 12 h. RNAiso Plus (Takara) was applied to extract total RNA of the samples. At least 2 µg of total RNA was added to synthesize cDNA, which was applied a PrimeScriptTM RT reagent Kit with gDNA Eraser (Takara). Quantitative RT-PCR was

carried out by applying Power SYBR Green PCR Master Mix (Applied Biosystems) on an ABI StepOneTM system (Applied Biosystems). 2^{-ΔΔCT} method was carried out to calculate the relative mRNA levels of gene tested and *cdc-42* was applied to the reference genes (37). The target gene expression in OP50 group was set as 1 for data normalization, *p* values were analyzed by using two tailed *t* test. The primers designed in this study are displayed in [Supplementary Table 13](#).

Western blotting assay

Synchronized L4 larvae N2 worms washed with PBS to clear residual bacteria were grown on plates with OP50 or *S. Paratyphi A* for 12 h. Worms (KU25 *pmk-1(km25) IV* was analyzed to verify mutant) were rinsed by PBS and then lysed in the RIPA buffer containing protease and phosphatase inhibitor mixture prior to triturating. BCA Protein Assay Kit (Beyotime) was applied to quantify the concentration of protein. After boiled, samples containing 20 µg proteins were separated on 12% SDS-PAGE and electro-transferred onto 0.2 µm polyvinylidene difluoride membranes. After blocked in 5% fat-free milk, The membranes were incubated with primary antibodies against phospho-p38/PMK-1 (1:1000, Cell Signaling) or actin (1:5000, Cell Signaling) followed by horseradish peroxidase-conjugated anti-mouse antibody (1:5000, Thermo Fisher Scientific). Quantification of blot were analyzed using Image J.

Results

S. Paratyphi A infection affected the phenotype of *C. elegans*

To test the effect of *S. Paratyphi A* infection on lifespan, we explored the lifespan of wild-type N2 hermaphrodites maintained at 25°C on agar plates with *E. coli* OP50 or *S. Paratyphi A*. Compared to OP50, *S. Paratyphi A* infection decreased the average mean lifespan of N2 by about 25% ([Figure 1A](#); [Supplementary Table 1](#)). Compared to other *E. coli* strains (HT115 and JM109), *S. Paratyphi A* also exhibited pathogenicity ([Supplementary Table 2](#)). Thermotolerance assay also indicated that *S. Paratyphi A* reduced the average mean lifespan of worms by up to 30% at 35°C ([Figure 1B](#); [Supplementary Table 1](#)). The higher temperature than normal is a stress factor by itself. To exclude the factor of heat stress, we also checked the lifespan of mutation of *hsf-1(sy441) I*, which carried the defect of heat shock factor. We found that the lifespan of the *hsf-1(sy441) I* mutant was significantly decreased when nematodes were exposed to *S. Paratyphi A* at 35°C ([Supplementary Table 3](#)). The mean hazard ratio for *hsf-1(sy441) I* mutant exposed to *S. Paratyphi A* were 6.557 compared to 6.706 of OP50 for the gene (Student's *t*-test *p*=0.55205). *S. Paratyphi A* infected worms may be independent of stress factor. Worms maintained at higher temperature achieved more distinct lethal effect, suggesting that 35°C was the optimum environment for *S. Paratyphi A* to infect the host. Body movement and reproduction

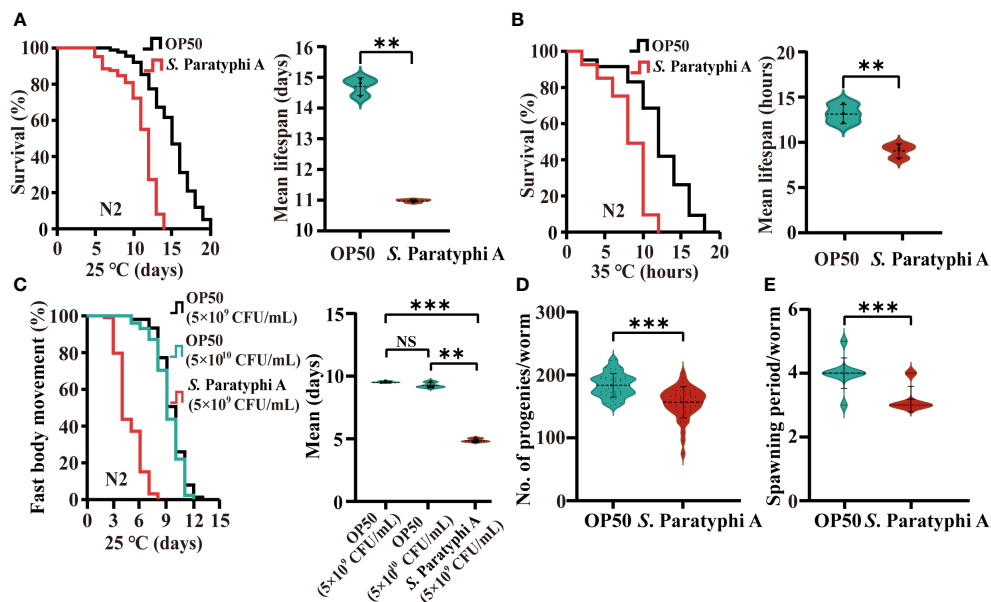


FIGURE 1

S. Paratyphi A reduced the lifespan and thermotolerance, shortened the period of fast body movement and reduced the reproductive capacity of *C. elegans*. (A) Representative survival curves of N2 of three independent trials and graphs of mean lifespan of at least 3 independent experiments at 25°C, and 35°C (B) on NGM plates containing either OP50 or *S. Paratyphi A*. Kaplan–Meier analysis was used to analyze the results of lifespan, and *p* values were calculated based on the log-rank test. Mean lifespans are presented as the mean \pm standard deviation. ** *p* < 0.01, Student's *t*-test. (C) Representative curves of three independent trials of age-related movements of worms treated with 5×10^9 and 5×10^{10} bacteria/mL for OP50 group and 5×10^9 bacteria/mL for *S. Paratyphi A* group (*p* < 0.0001, log-rank test) and graphs of mean fast movement period of at least 3 independent experiments (mean \pm SD, ** *p* < 0.01, *** *p* < 0.001, NS represents not significant, Student's *t*-test). The movements of nematodes were classified as fast and not fast movement. (D) Number of eggs laid (mean \pm SD, *** *p* < 0.001, Student's *t*-test) and spawning period (E) of worms cultured with OP50 and *S. Paratyphi A* (mean \pm SD, *** *p* < 0.001, Student's *t*-test).

were analyzed to check the physiological status of the worms. We analyzed the body movement of nematodes exposed to 5×10^9 and 5×10^{10} CFU/mL for OP50 and 5×10^9 CFU/mL for *S. Paratyphi A*, the bacteria density didn't lead to dieting (39) and also exclude the effect of thickness of the bacterial lawn caused by the slow growing of OP50. The results showed that 5×10^9 CFU/mL of *S. Paratyphi A* significantly shortened the period of fast body movement compared to 5×10^9 and 5×10^{10} CFU/mL of OP50 (Figure 1C; Supplementary Table 4). Furthermore, the number of eggs laying under the *S. Paratyphi A* treatment was reduced (OP50: 184 ± 19 eggs, *S. Paratyphi A*: 156 ± 25 eggs, *p* < 0.0001, Figure 1D; Supplementary Table 5). And the spawning period of worms was significantly shortened by *S. Paratyphi A* (OP50: 4 ± 0.5 days, *S. Paratyphi A*: 3.2 ± 0.4 days, *p* < 0.0001, Figure 1E; Supplementary Table 5).

S. Paratyphi A-trained worms indicated a strong bias for OP50, showed a decreased rate of pharyngeal pumping, and exhibited increased colonization in the intestinal tract.

C. elegans possess the capacity to perceive, recognize and escape pathogenic bacteria. Under laboratory conditions, the chemotaxis behavior of worms implied their food preference. Our results showed that worms maintained with *E. coli* OP50 did not exhibit

a bias to *E. coli* OP50 or *S. Paratyphi A* (chemotaxis index = 0.182 ± 0.055). However, nematodes trained on *S. Paratyphi A* for 12 h strongly preferred OP50 relative to pathogenic *S. Paratyphi A* (chemotaxis index = 0.677 ± 0.051 , *p* = 0.003203, Figure 2A; Supplementary Table 6). Pharyngeal pumping can reflect eating status. In general, when *C. elegans* were infected by pathogenic bacteria, they can reduce the bacteria intake to re-establish its behavior (40), therefore, we detected the number of pharyngeal pumps in 20s of nematode treated with OP50 or *S. Paratyphi A*. Our results showed that *S. Paratyphi A* exposure slowed the worms' pharyngeal pumping at 12 h (OP50: 43.9 ± 3.1 , *S. Paratyphi A*: 24.6 ± 2.9 , *p* < 0.0001), 24 h (OP50: 46.3 ± 4.1 , *S. Paratyphi A*: 27.5 ± 3.2 , *p* < 0.0001) or 48 h (OP50: 50.7 ± 4.5 , *S. Paratyphi A*: 35.4 ± 2.7 , *p* < 0.0001, Figure 2B; Supplementary Table 7). In general, *C. elegans* can respond to bacteria in the intestine and generate immune response to control the bacterial proliferation inside the body. Therefore, we also investigated whether *S. Paratyphi A* showed uncontrolled proliferation in the intestinal tract. Our results showed that the nematodes fed with *S. Paratyphi A* possessed more bacterial number than those fed *E. coli* OP50 for 12 h (OP50: 132 ± 37 CFU/worm, *S. Paratyphi A*: 2056 ± 534 CFU/worm, *p* < 0.0001), 24 h (OP50: 1066 ± 196 CFU/worm, *S. Paratyphi A*: 11622 ± 1029 CFU/worm, *p* < 0.0001) and 48 h (OP50: 3446 ± 316 CFU/worm, *S. Paratyphi A*: 379444 ± 28884 CFU/worm, *p* < 0.0001, Figure 2C; Supplementary Table 8). Fluorescence images of representative animals starved for 24 hours after feeding *E. coli*::eGFP or

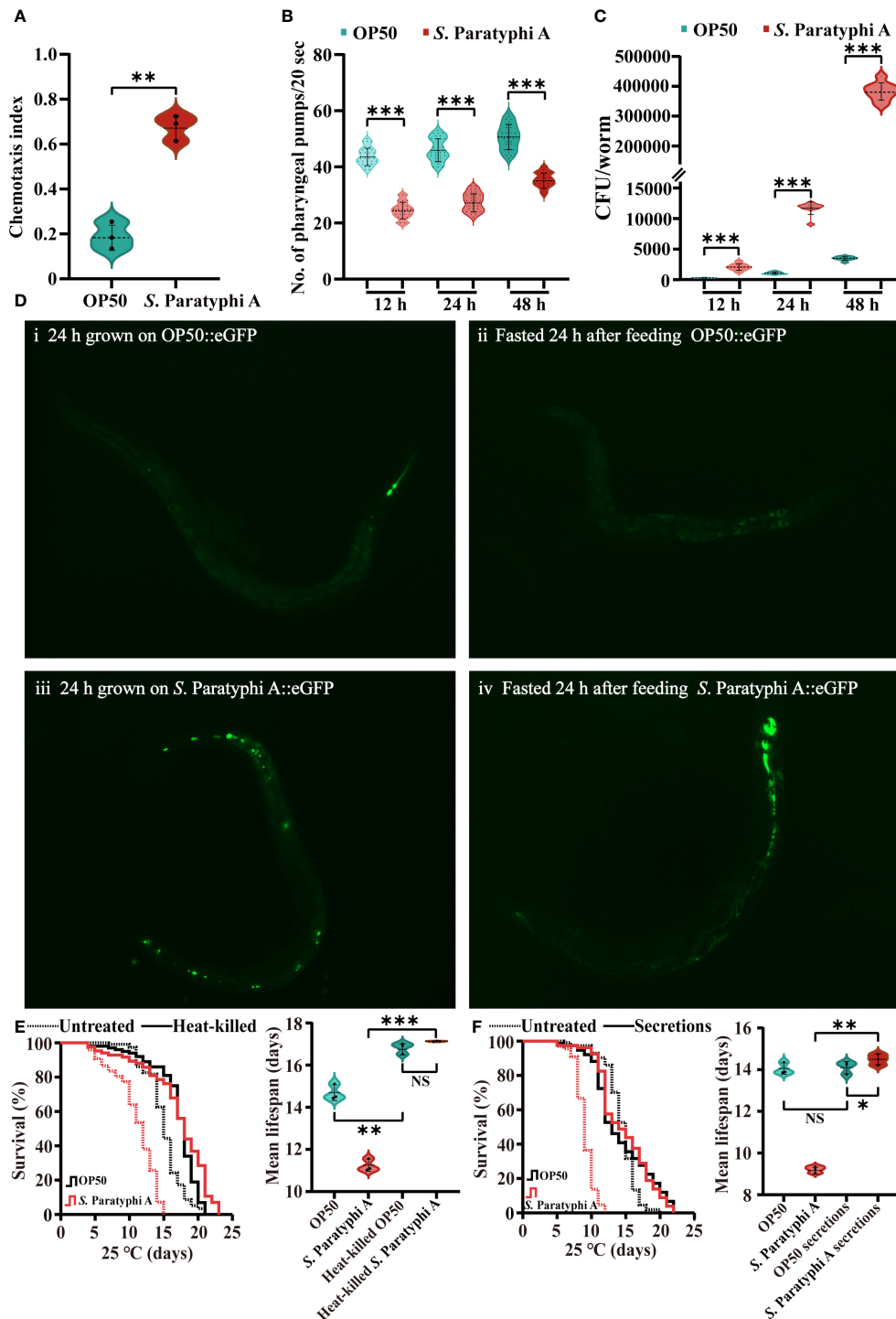


FIGURE 2

S. Paratyphi A-trained worms showed a bias toward OP50, a decreased rate of pharyngeal pumping, and increased colonization in the intestinal tract. (A) The chemotaxis index of wild-type N2 worms trained on OP50 or *S. Paratyphi A* (mean ± SD, ** $p < 0.01$, Student's *t*-test). (B) After 12 h, 24 h and 48 h of *S. Paratyphi A* infection, pharyngeal pumping assays were performed (mean ± SD, *** $p < 0.001$, Student's *t*-test). (C) The number of OP50 or *S. Paratyphi A* colonies/worm present in the intestine over 12 h (mean ± SD, *** $p < 0.001$), 24 h (mean ± SD, *** $p < 0.001$) and 48 h (mean ± SD, *** $p < 0.001$) treatment ($n=10$ in triplicates Student's *t*-test). (D) Fluorescence images of representative worms raised on *E. coli*::eGFP or *S. Paratyphi A*::eGFP (both carry the same eGFP expression plasmid). i Wild-type N2 worms fed *E. coli*::eGFP for 24 h. ii N2 worms fasted for 24 hours after feeding *E. coli*::eGFP. iii Wild-type N2 worms fed *S. Paratyphi A*::eGFP for 24 h. iv N2 worms fasted for 24 hours after feeding *S. Paratyphi A*::eGFP. (E) Representative survival curves (p value by log-rank test) and graphs of mean lifespan of at least 3 independent experiments (mean ± SD, $n=3$) of wild-type N2 worms on NGM plates containing untreated bacteria and heat-killed OP50 or *S. Paratyphi A*. OP50 (green) and *S. Paratyphi A* (red) show significantly lower survival and shorter mean lifespans compared to heat-killed controls (*** $p < 0.001$, Student's *t*-test). (F) Representative survival curves (p value by log-rank test) and graphs of mean lifespan of at least 3 independent experiments (mean ± SD, $n=3$) of wild-type N2 worms on NGM plates containing untreated bacteria and OP50 or *S. Paratyphi A* secretions. OP50 secretions (green) and *S. Paratyphi A* secretions (red) show significantly lower survival and shorter mean lifespans compared to untreated controls (* $p < 0.05$ and ** $p < 0.01$, NS represents not significant, Student's *t*-test).

S. Paratyphi A::eGFP further verified that *S. Paratyphi A* could proliferate in the intestinal lumen. After 24 hours of starvation, we observed evident fluorescence in *S. Paratyphi A*::eGFP-fasted animals but not in *E. coli*::eGFP-maintained or fasted worms (Figure 2D). We also discovered that the lifespan of worms showed no statistically significant differences between heat-killed *S. Paratyphi A* and OP50 bacteria (Figure 2E; Supplementary Table 9), and the lifespan of *S. Paratyphi A* secretions incubated with OP50 bacteria was similar to OP50 secretions (Figure 2F; Supplementary Table 10). The hazard ratios for heat-killed *S. Paratyphi A* and the secretions of living *S. Paratyphi A* were both reduced significantly. These results implied that the pathogenicity of *S. Paratyphi A* depends on living bacteria and is not mediated by secreting toxins.○

S. Paratyphi A-induced immune response in *C. elegans* requires activation of the MAPK pathway

To distinguish the signals involved in the interaction between *C. elegans* and *S. Paratyphi A*, we analyzed the lifespan of wild-type N2 and MAPK pathway mutants under exposure to *S. Paratyphi A*. The results showed that the mutants of *tir-1*, *nsy-1*, *sek-1* and *pmk-1* in the p38 MAPK pathway were more sensitive to *S. Paratyphi A* exposure than the wild type (Figures 3A–D, statistical information for all survival plots is presented in Supplementary Table 11). The *mpk-1* mutant in the ERK MAPK pathway also displayed greater sensitivity to *S. Paratyphi A* (Figure 3E; Supplementary Table 11). The results revealed that MAPK pathways function in the defense response of *C. elegans* to *S. Paratyphi A* infection. Reports have shown that the p38 MAPK pathway and *mpk-1* contribute to increase the nuclear localization of the transcription factor SKN-1 in the immune response (41, 42), therefore, we also detected the lifespan of wild-type N2 and the *skn-1(zu67)IV* mutant. We found that the lifespan of the *skn-1(zu67)IV* mutant was significantly decreased when nematodes were exposed to *S. Paratyphi A*, suggesting that *S. Paratyphi A* may activate the MAPK pathways in a SKN-1-dependent manner (Figure 3F; Supplementary Table 11). The hazard ratio for *tir-1*, *nsy-1*, *sek-1*, *pmk-1*, *mpk-1* and *skn-1* mutants exposed to *S. Paratyphi A* were higher than fed OP50 for these genes (Supplementary Table 11). We further confirmed the results by using quantitative RT-PCR to test the relative gene expression levels of *tir-1*, *nsy-1*, *sek-1*, *pmk-1*, *mpk-1*, and *skn-1* and the downstream target genes of SKN-1 (43) in the presence of *S. Paratyphi A*. The results showed that all these genes were upregulated when nematodes were exposed to *S. Paratyphi A* (Figure 3G; Supplementary Table 12). Considering activation of the p38 MAPK signaling pathway requires phosphorylation of p38 MAPK/PMK-1, we also compared the level of phosphorylated PMK-1 between *S. Paratyphi A* infection and OP50, the results displayed that *S. Paratyphi A* exposure has a higher level of activated P-p38/PMK-1 (Figure 3H), which further confirmed that MAPK pathways participated in the immune response of *C. elegans* to *S. Paratyphi A* exposure.

Defense against *S. paratyphi A* may require the participation of DAF-2 and DAF-16

Inhibited IIS could enhance immunity of *C. elegans*. We detected the lifespan of wild-type N2 and the mutant of *daf-2(e1370) III* under *S. Paratyphi A* infection, and the results indicated that the mean lifespan of *daf-2(e1370) III* did increase compared to that of the wild-type N2 after *S. Paratyphi A* treatment (Figure 4A; Supplementary Table 11). We also found a higher hazard ratio for *daf-2* mutant fed *S. Paratyphi A* than that for OP50 (Supplementary Table 11). The immune response of worms may require the regulation of *daf-2*. The DAF-2 downstream molecular DAF-16, which is homolog of FOXO in mammal, serves as a key node in immunity according to reports (25). We sought to determine whether DAF-16 was involved in *S. Paratyphi A* infection and found that the mutant of *daf-16* enhanced the susceptibility of worms to *S. Paratyphi A* (Figure 4B; Supplementary Table 11). The hazard ratio for *daf-16* mutant treated *S. Paratyphi A* was higher than that for OP50 (Supplementary Table 11). In addition, the results from transgenic strain T]356 zIs356 [*daf-16p::daf-16a/b::GFP + rol-6(su1006)*] indicated that *S. Paratyphi A* could significantly increase the nuclear localization of DAF-16 (Figure 4C; Supplementary Figure 2). We also analyzed the expression of *daf-16* and its downstream target genes *sod-3*, *hsp-12.6* and *dod-19* (44). The results indicated that *S. Paratyphi A* significantly upregulated the expression of *sod-3*, *hsp-12.6* and *dod-19* (Figure 4D; Supplementary Table 12). However, the level of *daf-16* didn't show great change. *S. Paratyphi A* may enhance the activity of DAF-16, instead of increasing the level of expression. These results suggested that DAF-16 was activated in worms to defend against *S. Paratyphi A*.

S. Paratyphi A may induce oxidative stress in *C. elegans*

Pathogenic bacteria can induce oxidative stress in worms (45), and oxidative stress could defend worms against *S. Paratyphi A* infection but also inevitably lead to tissue damage of host (46). Hydrogen peroxide, the familiar reactive oxygen molecules in worms, can destroy the function of cells directly or indirectly. As reported, pathogenic bacteria, such as *Streptococcus pyogenes*, could produce millimolar concentrations of hydrogen peroxide to infect and kill nematodes (47, 48). To determine the interaction mechanism between *C. elegans* and *S. Paratyphi A*, we performed hydrogen peroxide and quantitative RT-PCR assay. We found that the level of hydrogen peroxide after treatment with *S. Paratyphi A* for 12, 24 or 48 hours was significantly increased (Figure 5A; Supplementary Table 14). Quantitative RT-PCR assays also showed increasing expression of *ctl-1* and *ctl-3*, both involved in hydrogen peroxide catabolic process under *S. Paratyphi A* infection (Figure 5C; Supplementary Table 12), suggesting that *S. Paratyphi A* induced the production of hydrogen peroxide and increased oxidative stress. To further confirm that *S. Paratyphi A* induced a stress response in worms, we detected the expression changes of

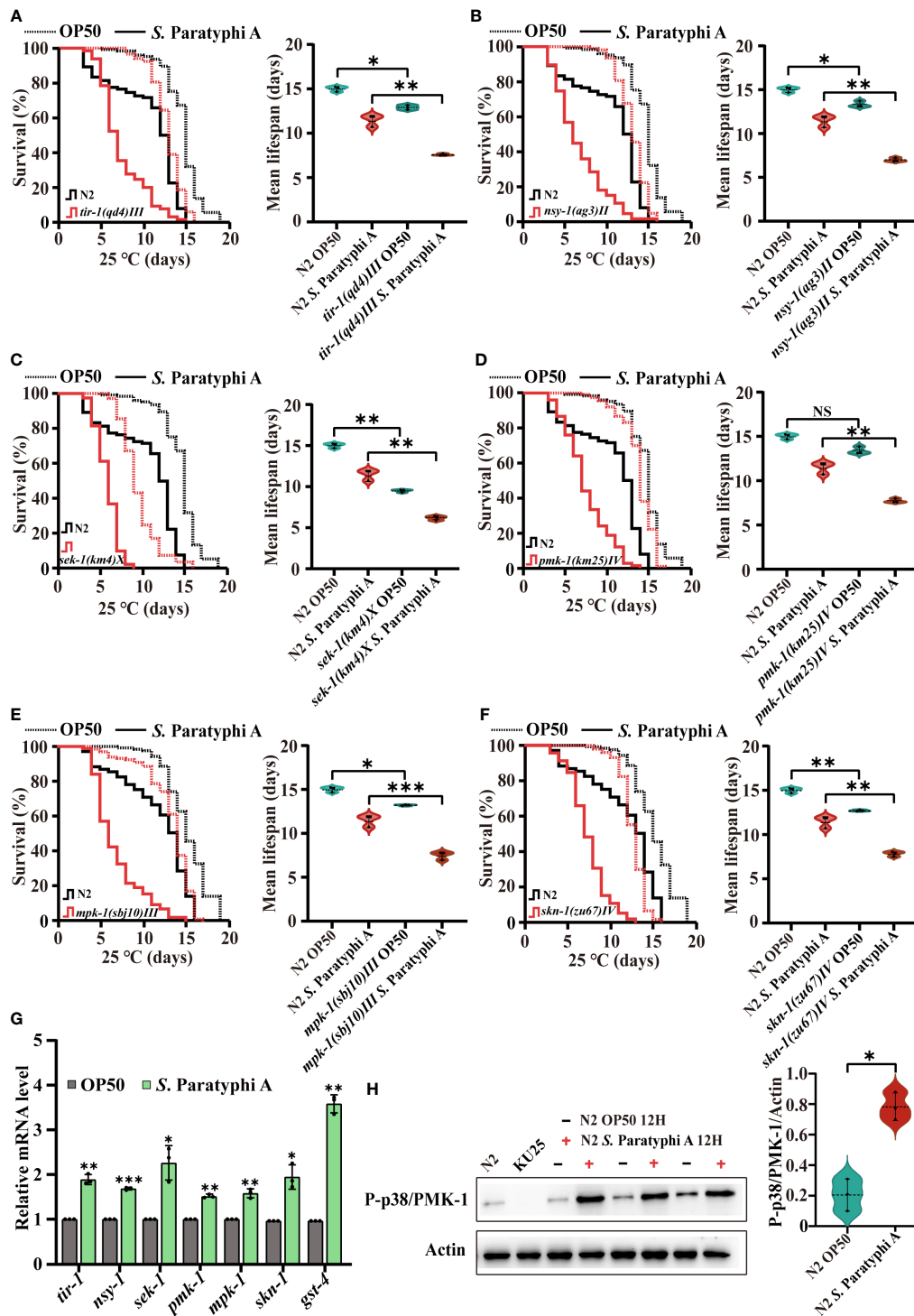


FIGURE 3

S. Paratyphi A-induced immune response in *C. elegans* requires activation of the MAPK pathway. Representative survival curves (*p* value by log-rank test) and graphs of mean lifespan of at least 3 independent experiments (mean \pm SD, * *p* < 0.05, ** *p* < 0.01, *** *p* < 0.001, NS represents not significant, Student's *t*-test) of wild-type N2 worms and mutants of *tir-1(qd4) III* (A), *nsy-1(ag3) II* (B), *sek-1(km4) X* (C), *pmk-1(km25) IV* (D), *mpk-1(sbj10) III* (E), *skn-1(zu67) IV* (F) on NGM plates containing OP50 or *S. Paratyphi A*. (G) Relative mRNA levels of *tir-1*, *nsy-1*, *sek-1*, *pmk-1*, *mpk-1*, and *skn-1* were detected by quantitative RT-PCR. Statistical analyses were calculated using two-tailed Student's *t*-test; * represents *p* < 0.05, ** represents *p* < 0.01, and *** represents *p* < 0.001. (H) Western blot analyses and quantify the level of P-p38 MAPK/PMK-1 in N2 worms treated OP50 or *S. Paratyphi A* (KU25 *pmk-1(km25) IV* was analyzed to verify mutant). Actin was displayed as the loading control (* *p* < 0.05, two-tailed Student's *t*-test).

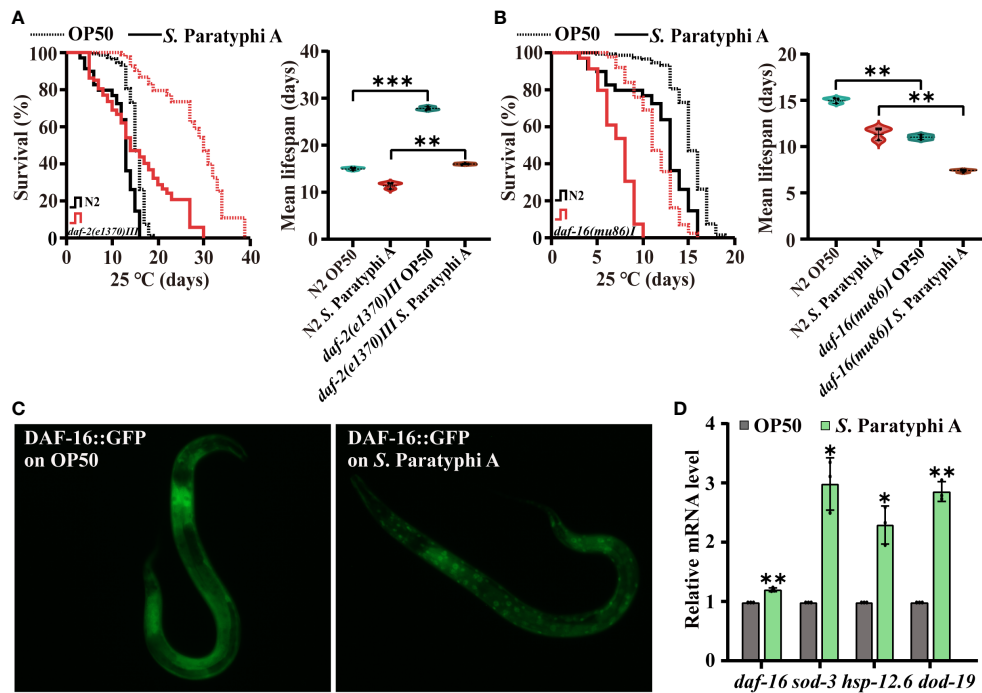


FIGURE 4

Defense against *S. Paratyphi A* may require the participation of DAF-2 and DAF-16. Representative survival curves (p value by log-rank test) and graphs of mean lifespan of at least 3 independent experiments (mean \pm SD, ** $p < 0.01$ and *** $p < 0.001$, Student's t -test) of wild-type N2 worms and mutants of *daf-2(e1370) III* (A) and *daf-16(mu86) I* (B). (C) Fluorescence images of TJ356 zls356 [*daf-16p::daf-16a/b::GFP* + *rol-6(su1006)*] grown on OP50 or *S. Paratyphi A* for 30 min. (D) Relative mRNA levels of *daf-16*, *sod-3*, *hsp-12.6* and *dod-19* were analyzed by quantitative RT-PCR (* $p < 0.05$ and ** $p < 0.01$, two-tailed Student's t -test).

stress response-related genes. We found that *asp-12*, *abf-2*, *abf-3*, *clec-186*, *dbl-1*, *clec-86*, *C32H11.4*, *ugt-63*, *spp-1*, *hsp-70* and *cyp-35A2* were upregulated when exposed to *S. Paratyphi A* (Figure 5C; Supplementary Table 12), while other stress response-related genes, including *lys-7*, *clec-174*, *clec-218*, *clec-258* and *clec-85* were downregulated (Figure 5B; Supplementary Table 12).

Discussion

S. Paratyphi A shortened the lifespan of *C. elegans* hermaphrodites maintained at 25°C and impaired the thermotolerance at 35°C. The maximal effect of infection appeared at 35°C, indicating that 35°C is an optimal temperature for *S. Paratyphi A* to attack organisms. 37°C is the optimal temperature for *S. Paratyphi A* grown, the virulence of the bacteria may almost rise to the highest level at 35°C. *S. Paratyphi A* infection causes phenotypical changes such as arresting pharynx and accelerating the decline in body movement. We observed that worms grown on *S. Paratyphi A* lawn showed a greater hesitation toward food intake, which led to slower pharyngeal pumping and body movement. Reproduction is one of the best indicators for organism fitness, *C. elegans* infected with *S. Paratyphi A* showed fewer eggs which suggest that *S. Paratyphi A* may affect reproductive capacity. In general, worms did not show a simultaneous preference for OP50 and *S. Paratyphi A*. However, *S. Paratyphi A*-trained worms presented strong preference to OP50 in the food choice experiment, which made it clear that worms had identified the perniciousness of *S. Paratyphi A* with training.

The CFU assay indicated that *S. Paratyphi A* colonized the intestinal region of *C. elegans*, and the fluorescence intensity in the intestine lumen further confirmed that *S. Paratyphi A* infect *C. elegans* through rapid proliferation in the intestinal tract. *S. Paratyphi A* colonizes the intestine and may have an effect on the locomotion and pharyngeal pumping rates of *C. elegans*. Our results confirmed that *S. Paratyphi A* can infect *C. elegans* and has an effect on phenotypic changes in worms. As the lifespan of secretions and heat-killed treatment of *S. Paratyphi A* showed no significant different from that of OP50 bacteria, the pathogenic bacteria mainly infect through colonizing the intestinal region.

MAPK is a conserved pathway in *C. elegans* innate immunity and is essential for defending worms against pathogens such as *Pseudomonas aeruginosa*, *Cutibacterium acnes*, *Yersinia pestis*, and opportunistic *Proteus* species (49–52). In this study, the p38 MAPK and ERK MAPK pathway mutants showed greater sensitivity to *S. Paratyphi A* exposure than the wild type and higher hazard ratio to OP50, indicating that MAPK pathways may be activated in the immune response of *C. elegans* to *S. Paratyphi A* infection, and the higher level of phosphorylated PMK-1 in *S. Paratyphi A* infection obtained by western blot further confirmed the conclusion. The lifespan results of the *skn-1(zu67) IV* mutant verified that SKN-1 was involved in the defense response of *C. elegans* and may be activated by MAPK or oxidative stress, which will be further verified. These results were also obtained by quantitative RT-PCR. The long-lived *daf-2(e1370) III* showed a lifespan longer to that of the wild type under *S. Paratyphi A* exposure, and the expression of *daf-2* in *S. Paratyphi A*

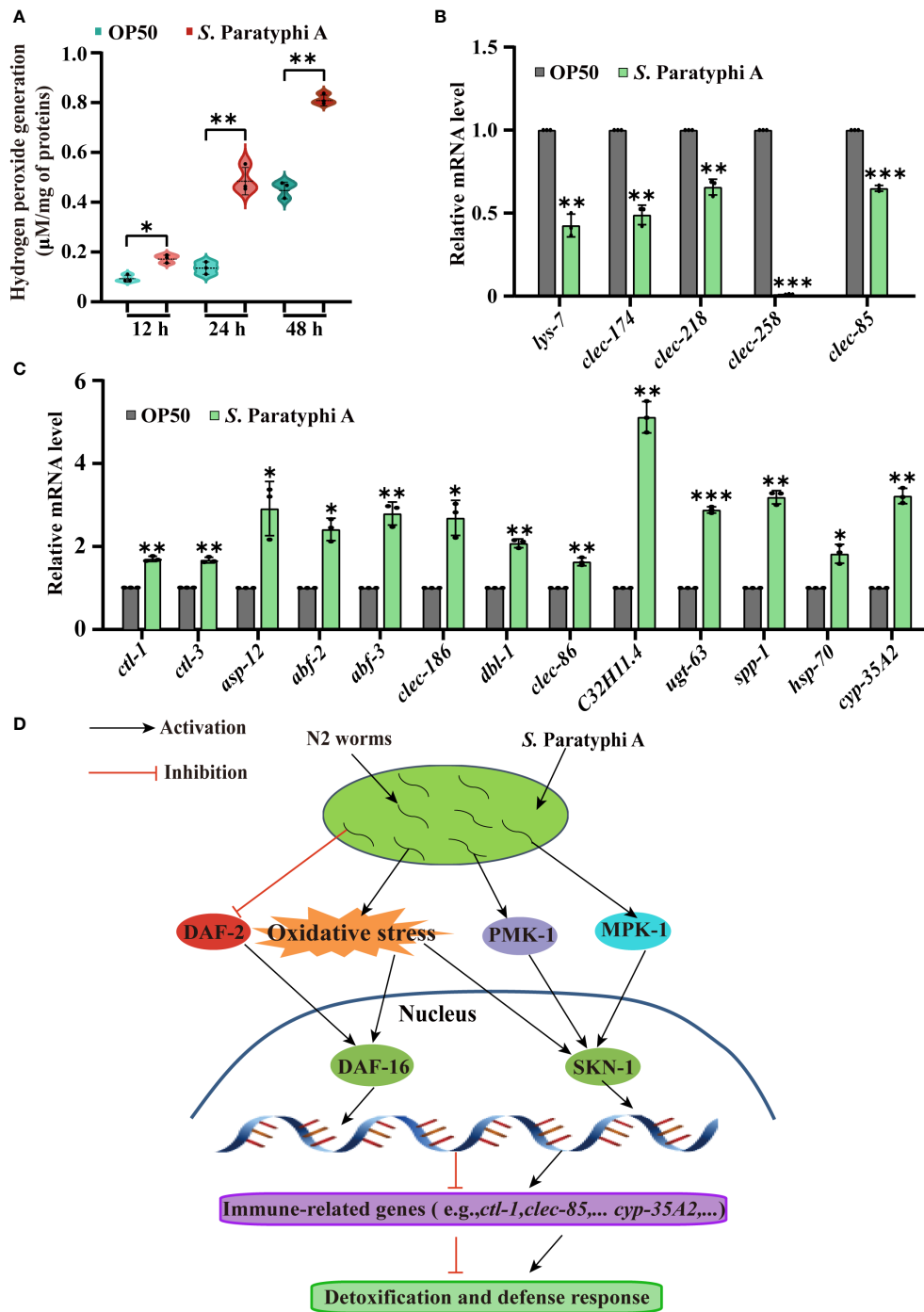


FIGURE 5
 Stress response changes in *C. elegans* exposed to *S. Paratyphi A*. (A) Hydrogen peroxide assay after treatment with OP50 or *S. Paratyphi A* for 12, 24 or 48 hours (mean ± SD, * $p < 0.05$ and ** $p < 0.01$, Student's *t*-test). (B) Relative mRNA levels of stress response-related genes *lys-7*, *clec-174*, *clec-218*, *clec-258*, *clec-85* and (C) *ctl-1*, *ctl-3*, *asp-12*, *abf-2*, *abf-3*, *clec-186*, *dbl-1*, *clec-86*, *C32H11.4*, *ugt-63*, *spp-1*, *hsp-70* and *cyp-35A2* were analyzed by quantitative RT-PCR (* $p < 0.05$, ** $p < 0.01$, *** $p < 0.001$, two-tailed Student's *t*-test). (D) Model of the interaction between *S. Paratyphi A* and *C. elegans*.

infect displayed slightly downregulated (Supplementary Table 12) indicated that inhibition of insulin signaling may defend worms against *S. Paratyphi A* infection. However, we also detected a higher hazard ratio for *daf-2* mutant in *S. Paratyphi A*, as *daf-2(e1370) III* is partially defective and extremely longevity, the effect of *daf-2* mutant fed *S. Paratyphi A* may ascribe complex signal regulation or other

factors produced by *S. Paratyphi A*, which needs further exploration. The transcription factor DAF-16 of *C. elegans* integrate upstream signals to regulate the transcription of many genes related to stress, metabolism, and immunity (25). As reported, DAF-16 could be activated by *Bacillus thuringiensis*, *Pseudomonas aeruginosa*, *Cryptococcus neoformans* and *Cryptococcus gattii* infections (53–55).

Our results found that the mutant *daf-16(mu86)I* enhanced susceptibility to *S. Paratyphi A* infection in *C. elegans* and the nuclear localization of DAF-16::GFP were enhanced in *S. Paratyphi A* exposure. All these results verify that worms activate DAF-16 to defend against *S. Paratyphi A*, and the increase in the expression of *sod-3*, *hsp-12.6* and *dod-19* confirmed this speculation. DAF-16 can be regulated by a variety of upstream signals, such as the typical IIS (56) and oxidative stress (25). Because *S. Paratyphi A* may regulate insulin signaling and stress response, DAF-16 may be activated by these signals (Figure 5D).

Oxidative stress also plays a crucial role in pathogen infection. The increase in the level of hydrogen peroxide after exposure to *S. Paratyphi A* confirmed that the oxidative stress response was involved in the interaction between *S. Paratyphi A* and *C. elegans*. The quantitative RT-PCR data indicated that the interaction between *S. Paratyphi A* and *C. elegans* was particularly enriched in the stress response. *C. elegans* upregulated genes related to the immune response to attack bacteria, while *S. Paratyphi A* downregulated certain detoxification genes so that they could colonize the worms.

In this study, we found that *S. Paratyphi A* could shorten the lifespan of *C. elegans* and cause phenotypical changes mainly by colonizing the intestinal region and regulating the stress response. MAPK and DAF-16 played a central role in *C. elegans* defense against *S. Paratyphi A*. Our findings revealed the interaction between *S. Paratyphi A* and *C. elegans* and provided insights for the development of novel pharmaceutical agents targeting bacterial infectious diseases.

Data availability statement

The raw data supporting the conclusions of this article will be made available by the authors, without undue reservation.

Author contributions

W-KZ and A-JD conceived the study. A-JD, X-CL, YD, H-JM, S-DP did most of the experiments. W-MZ, JT, BC and J-BH

contributed to part of materials. W-KZ and A-JD wrote the manuscript. All authors contributed to the article and approved the submitted version.

Funding

This work was supported by the [Natural Science Foundation of China#1] under Grant [Nos. 82060668 and 31960033]; [Joint Special Project of Universities in Yunnan Province#2] under Grant [Nos. 2018FH001-095 and 2018FH001-005]; [Talent Introduction Project of Kunming University#3] under Grant [Nos. YJL18013] and [Spring City Project#4] under Grant [Nos.C201914001].

Conflict of interest

The authors declare that the research was conducted in the absence of any commercial or financial relationships that could be construed as a potential conflict of interest.

Publisher's note

All claims expressed in this article are solely those of the authors and do not necessarily represent those of their affiliated organizations, or those of the publisher, the editors and the reviewers. Any product that may be evaluated in this article, or claim that may be made by its manufacturer, is not guaranteed or endorsed by the publisher.

Supplementary material

The Supplementary Material for this article can be found online at: <https://www.frontiersin.org/articles/10.3389/fimmu.2023.1118003/full#supplementary-material>

References

- Dunne JA, Wilson J, Gokhale J. Small bowel perforation secondary to enteric salmonella paratyphi a infection. *BMJ Case Rep* (2011) 2011:bcr0820103272. doi: 10.1136/bcr.08.2010.3272
- Manesh A, Meltzer E, Jin C, Britto C, Deodhar D, Radha S, et al. Typhoid and paratyphoid fever: a clinical seminar. *J Travel Med* (2021) 28:taab012. doi: 10.1093/jtm/taab012
- Lu X, Li Z, Yan M, Pang B, Xu J, Kan B. Regional transmission of salmonella paratyphi a, china 1998-2012. *Emerg Infect Dis* (2017) 23:833-6. doi: 10.3201/eid2305.151539
- Arndt MB, Mosites EM, Tian M, Forouzanfar MH, Mokhdad AH, Meller M, et al. Estimating the burden of paratyphoid a in Asia and Africa. *PLoS Negl Trop Dis* (2014) 8:e2925. doi: 10.1371/journal.pntd.0002925
- Siddiqui FJ, Rabbani F, Hasan R, Nizami SQ, Bhutta ZA. Typhoid fever in children: some epidemiological considerations from Karachi, Pakistan. *Int J Infect Dis* (2006) 10:215-22. doi: 10.1016/j.ijid.2005.03.010
- Bhattacharya SS, Satapathi S. A sudden increase in occurrence of salmonella paratyphi a infection in rourkela, western odisha. *Trop Doct* (2019) 49:323-4. doi: 10.1177/0049475519863214
- Feng Y, Chen YC, Janapatla RP, Wang Z, Hsu YJ, Chen CL, et al. Genomic surveillance reveals international circulation and local transmission of salmonella enterica serovars typhi and paratyphi a in Taiwan. *J Microbiol Immunol Infect* (2021) 55:489-93. doi: 10.1016/j.jmii.2021.06.004
- Pan P, Zou F, He C, He Q, Yin J. Characterization and protective efficacy of a sPT mutant of salmonella paratyphi a. *Immun Inflammation Dis* (2020) 8:774-81. doi: 10.1002/iid3.369
- Li P, Zhang K, Lei T, Zhou Z, Luo H. Multiple immunodominant O-epitopes co-expression in live attenuated salmonella serovars induce cross-protective immune responses against s. paratyphi a, s. typhimurium and s. enteritidis. *PLoS Negl Trop Dis* (2022) 16:e0010866. doi: 10.1371/journal.pntd.0010866
- Das S, Chowdhury R, Pal A, Okamoto K, Das S. Salmonella typhi outer membrane protein STIV is a potential candidate for vaccine development against typhoid and paratyphoid fever. *Immunobiology* (2019) 224:371-82. doi: 10.1016/j.imbio.2019.02.011
- Vij S, Thakur R, Kumari L, Suri CR, Rishi P. Potential of a novel flagellin epitope as a broad-spectrum vaccine candidate against enteric fever. *Microb Pathog* (2023) 174:105936. doi: 10.1016/j.micpath.2022.105936

12. Sun P, Pan C, Zeng M, Liu B, Liang H, Wang D, et al. Design and production of conjugate vaccines against *S. paratyphi* A using an O-linked glycosylation system *in vivo*. *NPJ Vaccines* (2018) 3:4. doi: 10.1038/s41541-017-0037-1
13. Dhara D, Baliban SM, Huo CX, Rashidjahanabad Z, Sears KT, Nick ST, et al. Syntheses of salmonella paratyphi A associated oligosaccharide antigens and development towards anti-paratyphoid fever vaccines. *Chemistry* (2020) 26:15953–68. doi: 10.1002/chem.202002401
14. Bhattacharya SS, Das U, Choudhury BK. Occurrence & antibiogram of salmonella typhi & *S. paratyphi* A isolated from rourkela, orissa. *Indian J Med Res* (2011) 133:431–3.
15. Meltzer E, Stienlauf S, Leshem E, Sidi Y, Schwartz E. A Large outbreak of salmonella paratyphi A infection among Israeli travelers to Nepal. *Clin Infect Dis* (2013) 58:359–64. doi: 10.1093/cid/cit723
16. Prabhurajan R, Selvam RME, Padmavathy K. Unusual antibiotic resistance pattern among blood culture isolates of salmonella paratyphi A. *J Infect Dev Ctries* (2021) 15:579–83. doi: 10.3855/jidc.12336
17. Manoharan A, Dey D, Putlibai S, Ramaiah S, Anbarasu A, Balasubramanian S. Epidemiology of multidrug resistance among salmonella enterica serovars typhi and paratyphi A at a tertiary pediatric hospital in India over a decade; in-silico approach to elucidate the molecular mechanism of quinolone resistance. *Int J Infect Dis* (2022) 119:146–9. doi: 10.1016/j.ijid.2022.03.050
18. Kumar A, Baruah A, Tomioka M, Iino Y, Kalita MC, Khan M. Caenorhabditis elegans: a model to understand host-microbe interactions. *Cell Mol Life Sci* (2020) 77:1229–49. doi: 10.1007/s00018-019-03319-7
19. Zhang R, Hou A. Host-microbe interactions in caenorhabditis elegans. *ISRN Microbiol* (2013) 2013:356451. doi: 10.1155/2013/356451
20. Cohen LB, Troemel ER. Microbial pathogenesis and host defense in the nematode *C. elegans*. *Curr Opin Microbiol* (2015) 23:94–101. doi: 10.1016/j.mib.2014.11.009
21. Dinić M, Jakovljević S, Đokić J, Popović N, Radojević D, Strahinić I, et al. Probiotic-mediated p38 MAPK immune signaling prolongs the survival of caenorhabditis elegans exposed to pathogenic bacteria. *Sci Rep* (2021) 11:21258. doi: 10.1038/s41598-021-00698-5
22. Wan J, Yuan L, Jing H, Zheng Q, Xiao H. Defective apoptotic cell clearance activates innate immune response to protect caenorhabditis elegans against pathogenic bacteria. *Virulence* (2021) 12:75–83. doi: 10.1080/21505594.2020.1857982
23. Evans EA, Chen WC, Tan MW. The DAF-2 insulin-like signaling pathway independently regulates aging and immunity in *C. elegans*. *Aging Cell* (2008) 7:879–93. doi: 10.1111/j.1474-9726.2008.00435.x
24. Riera CE, Merkwirth C, De Magalhaes Filho CD, Dillin A. Signaling networks determining life span. *Annu Rev Biochem* (2016) 85:35–64. doi: 10.1146/annurev-biochem-060815-014451
25. Zecic A, Braeckman BP. DAF-16/FoxO in caenorhabditis elegans and its role in metabolic remodeling. *Cells* (2020) 9:109. doi: 10.3390/cells9010109
26. Duangjan C, Rangsinth P, Gu X, Zhang S, Wink M, Tencomnao T. Glochidion zeylanicum leaf extracts exhibit lifespan extending and oxidative stress resistance properties in caenorhabditis elegans via DAF-16/FoxO and SKN-1/Nrf-2 signaling pathways. *Phytomedicine* (2019) 64:153061. doi: 10.1016/j.phymed.2019.153061
27. Li SW, Huang CW, Liao VH. Early-life long-term exposure to ZnO nanoparticles suppresses innate immunity regulated by SKN-1/Nrf and the p38 MAPK signaling pathway in caenorhabditis elegans. *Environ pollut* (2020) 256:113382. doi: 10.1016/j.envpol.2019.113382
28. Brenner S. The genetics of caenorhabditis elegans. *Genetics* (1974) 77:71–94. doi: 10.1093/genetics/77.1.71
29. Hosono R, Mitsui Y, Sato Y, Aizawa S, Miwa J. Life span of the wild and mutant nematode caenorhabditis elegans. effects of sex, sterilization, and temperature. *Exp Gerontol* (1982) 17:163–72. doi: 10.1016/0531-5565(82)90052-3
30. White CV, Darby BJ, Breeden RJ, Herman MA, Payne SM. A stenotrophomonas maltophilia strain evades a major caenorhabditis elegans defense pathway. *Infection Immun* (2016) 84:524–36. doi: 10.1128/iai.00711-15
31. Wilson MA, Shukitt-Hale B, Kalt W, Ingram DK, Joseph JA, Wolkow CA. Blueberry polyphenols increase lifespan and thermotolerance in caenorhabditis elegans. *Aging Cell* (2006) 5:59–68. doi: 10.1111/j.1474-9726.2006.00192.x
32. Ding AJ, Wu GS, Tang B, Hong X, Zhu MX, Luo HR. Benzimidazole derivative M084 extends the lifespan of caenorhabditis elegans in a DAF-16/FOXO-dependent way. *Mol Cell Biochem* (2017) 426:101–9. doi: 10.1007/s11010-016-2884-x
33. Moore RS, Kaletsky R, Murphy CT. Piwi/PRG-1 argonaute and TGF-beta mediate transgenerational learned pathogenic avoidance. *Cell* (2019) 177:1827–1841.e1812. doi: 10.1016/j.cell.2019.05.024
34. Portal-Celhay C, Bradley ER, Blaser MJ. Control of intestinal bacterial proliferation in regulation of lifespan in caenorhabditis elegans. *BMC Microbiol* (2012) 12:49. doi: 10.1186/1471-2180-12-49
35. Xiao Y, Wang P, Zhu X, Xie Z. Pseudomonas donghuensis HYS gtrA/B/II gene cluster contributes to its pathogenicity toward caenorhabditis elegans. *Int J Mol Sci* (2021) 22:10741. doi: 10.3390/ijms221910741
36. Gravato-Nobre MJ, Vaz F, Filipe S, Chalmers R, Hodgkin J. The invertebrate lysozyme effector ILYS-3 is systemically activated in response to danger signals and confers antimicrobial protection in *C. elegans*. *PLoS Pathog* (2016) 12:e1005826. doi: 10.1371/journal.ppat.1005826
37. Zheng SQ, Huang XB, Xing TK, Ding AJ, Wu GS, Luo HR. Chlorogenic acid extends the lifespan of caenorhabditis elegans via Insulin/IGF-1 signaling pathway. *J Gerontol A Biol Sci Med Sci* (2017) 72:464–72. doi: 10.1093/gerona/glw105
38. Kaletsky R, Moore RS, Vrla GD, Parsons LR, Gitai Z, Murphy CT. K. C. elegans interprets bacterial non-coding RNAs to learn pathogenic avoidance. *Nature* (2020) 586:445–51. doi: 10.1038/s41586-020-2699-5
39. Kim SH, Kim BK, Park SK. Selenocysteine mimics the effect of dietary restriction on lifespan via SKN1 and retards age-associated pathophysiological changes in caenorhabditis elegans. *Mol Med Rep* (2018) 18:389–5398. doi: 10.3892/mmr.2018.9590
40. Ooi SK, Lim TY, Lee SH, Nathan S. Burkholderia pseudomallei kills caenorhabditis elegans through virulence mechanisms distinct from intestinal lumen colonization. *Virulence* (2012) 3:485–96. doi: 10.4161/viru.21808
41. Inoue H, Hisamoto N, An JH, Oliveira RP, Nishida E, Blackwell TK, et al. The *C. elegans* p38 MAPK pathway regulates nuclear localization of the transcription factor SKN-1 in oxidative stress response. *Genes Dev* (2005) 19:2278–83. doi: 10.1101/gad.1324805
42. Yoon DS, Cha DS, Choi Y, Lee JW, Lee MH. MPK-1/ERK is required for the full activity of resveratrol in extended lifespan and reproduction. *Aging Cell* (2019) 18:e12867. doi: 10.1111/acel.12867
43. Song B, Zheng B, Li T, Liu RH. SKN-1 is involved in combination of apple peels and blueberry extracts synergistically protecting against oxidative stress in caenorhabditis elegans. *Food Funct* (2020) 11:5409–19. doi: 10.1039/d0fo00891e
44. Yasuda K, Kubo Y, Murata H, Sakamoto K. Cortisol promotes stress tolerance via DAF-16 in caenorhabditis elegans. *Biochem Biophys Res* (2021) 26:100961. doi: 10.1016/j.bbrep.2021.100961
45. Li D, Deng Y, Wang S, Du H, Xiao G, Wang D. Assessment of nanoplastyrene toxicity under fungal infection condition in caenorhabditis elegans. *Ecotoxicol Environ Saf* (2020) 197:110625. doi: 10.1016/j.ecoenv.2020.110625
46. Hoeven R, McCallum KC, Cruz MR, Garsin DA. Ce-Duox1/BLI-3 generated reactive oxygen species trigger protective SKN-1 activity via p38 MAPK signaling during infection in *C. elegans*. *PLoS Pathog* (2011) 7:e1002453. doi: 10.1371/journal.ppat.1002453
47. Jansen WT, Bolm M, Balling R, Chhatwal GS, Schnabel R. Hydrogen peroxide-mediated killing of caenorhabditis elegans by streptococcus pyogenes. *Infect Immun* (2002) 70:5202–7. doi: 10.1128/iai.70.9.5202-5207.2002
48. Schiffer JA, Stumber SV, Seyedolmohadesin M, Xu Y, Serkin WT, McGowan NG, et al. Modulation of sensory perception by hydrogen peroxide enables caenorhabditis elegans to find a niche that provides both food and protection from hydrogen peroxide. *PLoS Pathog* (2021) 17:e1010112. doi: 10.1371/journal.ppat.1010112
49. Kim DH, Fienbaum R, Allogio G, Emerson FE, Garsin DA, Inoue H, et al. A conserved p38 MAPK kinase pathway in caenorhabditis elegans innate immunity. *SCIENCE* (2002) 297:623–6. doi: 10.1126/science.1073759
50. Bolz DD, Tenor JL, Aballay A. A conserved PMK-1/p38 MAPK is required in caenorhabditis elegans tissue-specific immune response to yersinia pestis infection. *J Biol Chem* (2010) 285:10832–40. doi: 10.1074/jbc.M109.091629
51. Jebamercy G, Vigneshwari L, Balamurugan K. A MAP kinase pathway in caenorhabditis elegans is required for defense against infection by opportunistic Proteus species. *Microbes Infect* (2013) 15:550–68. doi: 10.1016/j.micinf.2013.03.009
52. Tsuru A, Hamazaki Y, Tomida S, Ali MS, Kage-Nakadai E. The defense response of caenorhabditis elegans to cutibacterium acnes SK137 via the TIR-1-p38 MAPK signaling pathway. *Bioscience Biotechnol Biochem* (2022) 86:374–9. doi: 10.1093/bbb/zbab218
53. Wang J, Nakad R, Schulenburg H. Activation of the caenorhabditis elegans FOXO family transcription factor DAF-16 by pathogenic bacillus thuringiensis. *Dev Comp Immunol* (2012) 37:193–201. doi: 10.1016/j.dci.2011.08.016
54. Mchugh DR, Koumis E, Jacob P, Goldfarb J, Schlaubitz-Garcia M, Bennani S, et al. DAF-16 and SMK-1 contribute to innate immunity during adulthood in caenorhabditis elegans. *G3 (Bethesda)* (2020) 10:1521–39. doi: 10.1534/g3.120.401166
55. Kitisin T, Muangkaew W, Sukphopetch P. Caenorhabditis elegans DAF-16 regulates lifespan and immune responses to cryptococcus neoformans and cryptococcus gattii infections. *BMC Microbiol* (2022) 22(1):162. doi: 10.1186/s12866-022-02579-x
56. Xiao X, Zhou Y, Tan C, Bai J, Zhu Y, Zhang J, et al. Barley β -glucan resist oxidative stress of caenorhabditis elegans via daf-2/daf-16 pathway. *Int J Biol Macromol* (2021) 193:1021–31. doi: 10.1016/j.ijbiomac.2021.11.067